Study of the shape of random walks. II. Inertia moment ratios and the two-dimensional asphericity

1995 J. Phys. A: Math. Gen. 28 3667

(http://iopscience.iop.org/0305-4470/28/13/012)

J. Phys. A: Math. Gen. 28 (1995) 3667–3679. Printed in the UK

Study of the shape of random walks: II. Inertia moment ratios and the two-dimensional asphericity

S J Sciutto†

Laboratorio de Física Teórica, Departamento de Física, Universidad Nacional de La Plata, CC 67–1900 La Plata, Argentina

Received 19 January 1995

Abstract. A study of some features of the quantities used to describe the shape of random walks, focusing on the probability distribution of the asphericity of discrete random walks in two dimensions, is presented. A connection is established between the asphericity distribution and the probability distribution corresponding to the ratio of the principal inertia moments. The probability distributions of arbitrary inertia moment ratios are analysed for varying spatial dimension, and an analytic expression for them is found which presents excellent agreement with Monte Carlo data in all the cases considered. This function is then used to obtain the corresponding two-dimensional asphericity distribution, which also proved to be a very good approximation to the true distribution obtained from an independent Monte Carlo simulation.

1. Introduction

In a recent paper [1] we presented a comprehensive study of the shapes of discrete unrestricted random walks in d dimensions. In that paper we discussed the probability distribution of several quantities, namely, the principal inertia moments, the asphericity [1–3] and the angle between the principal axis of inertia and the end-to-end vector [1, 4].

We also found an analytical probability distribution for the inertia eigenvalues which approximates the Monte Carlo data very well in a number of cases, and have used it to construct the corresponding combined probability distribution in order to obtain analytical expressions for derived quantities such as the asphericity. Among other results, it was established that the resulting probability distribution for the asphericity in two-dimensional spaces disagrees significantly from the true one [1].

As mentioned in [1], the study of the shape of random walks is of interest to many scientists, especially (but not reduced to) those connected with polymer science. For example, the concept of the shape of random walks has recently been used to analyse the effect of the concentration [5] or interactions [6] on the mean dimensions of single polymer chain models. In this paper we are going to present a study of some properties of the asphericity and related quantities which we consider will be useful to applications like the ones already cited.

The main scope of this work is to present a more complete analysis of the probability distribution of the asphericity in two dimensions. To this end we establish a connection between the asphericity distribution and the probability distribution of ratios of inertia moments. Then we find an analytical expression for such distributions which presents

† E-mail address: sciutto@venus.fisica.unlp.edu.ar

0305-4470/95/133667+13$19.50

an excellent agreement with the distributions obtained from Monte Carlo simulations. The expression found possesses four external parameters which are set by nonlinear least-squares fits with the respective Monte Carlo data.

The distribution mentioned is used to obtain an analytical probability distribution for the asphericity in two-dimensional spaces, and this distribution is, in turn, checked against the distribution obtained from an independent Monte Carlo simulation, finding that there is a very good degree of agreement between both curves.

There exist previous papers which study some related quantities such as the ratios of *mean values* of inertia moments [4, 7] of three-dimensional random walks, combinations of some of these mean values in connection with the asphericity [2, 8], and/or probability distributions for the three-dimensional asphericity [3]. To the best of our knowledge, and excluding our previous paper [1], there are no other studies of the quantities analysed in the paper, that is, probability distributions of the two-dimensional asphericity and/or inertia moment ratios in spaces of arbitrary dimension.

Our paper is organized as follows. In section 2 we present most of the definitions and basic formulae that will be used throughout this paper. In section 3 we address the problem of the asphericity in two dimensions, review some results of [1] and establish the connection with the moment ratios. In section 4 we present a detailed study of the probability distribution of the inertia moment ratios for arbitrary spatial dimension. In section 5 we return to the asphericity, analysing the probability distribution that is obtained combining the results of sections 3 and 4. Finally, in section 6 we give our conclusions and final remarks.

2. Definitions

A random walk of s steps in a d-dimensional space can be defined by specifying $s+1$ d-dimensional vectors r_α, $\alpha = 0, \ldots, s$, which represent the positions within the walk [1]. With no loss of generality we will take $r_0 = 0$. We also introduce the step vectors:

$$r_\alpha = r_{\alpha-1} + \epsilon_\alpha \qquad \alpha = 1, \ldots, s\,. \tag{1}$$

For discrete unrestricted random walks with coordination number $2d$, each one of the vectors ϵ_α may be any one of the unitary vectors $\pm e_1, \pm e_2, \ldots, \pm e_d$, where $B = \{e_1, \ldots, e_d\}$ is an orthonormal basis of the d-dimensional space.

To obtain an adequate measure of the shape of a random walk, we use the following quantities [1]:

(i) The *centre of mass*:

$$r_{\mathrm{CM}} = \frac{1}{s+1}\sum_{\alpha=1}^{s} r_\alpha\,. \tag{2}$$

(ii) The *inertia matrix*:

$$T_{ij} = \frac{1}{s+1}\sum_{\alpha=0}^{s}(x_{i\alpha} - x_{\mathrm{CM}i})(x_{j\alpha} - x_{\mathrm{CM}j}) \qquad 1 \leqslant i \leqslant d \qquad 1 \leqslant j \leqslant d\,. \tag{3}$$

This matrix is symmetric and positive definite. It possesses d positive eigenvalues $\lambda_1 \geqslant \lambda_2 \geqslant \cdots \geqslant \lambda_d$, and an orthogonal set of d eigenvectors.

(iii) The *asphericity*:

$$A = \frac{1}{d-1}\left[d\left(\sum_{i=1}^{d}\lambda_i^2\right)\left(\sum_{i=1}^{d}\lambda_i\right)^{-2} - 1\right]. \tag{4}$$

This quantity takes values between 0 and 1. $A = 0$ (1) corresponds to a perfectly spherical (rod) shape [1, 2].

In a computer simulation, statistically independent random walks of a given length s are generated. In general, this provides a set of random walks with different shapes, which can be used to build frequency histograms for quantities such as the asphericity and the principal inertia moments.

Here let us introduce the probability distribution for the principal inertia moments: let $r = \min(d, s)$, the eigenvalues λ_k, $k = 1, \ldots, r$ distribute accordingly with $P_k(\lambda)$, which verifies the normalization condition $\int_0^\infty P_k(\lambda)\,d\lambda = 1$. In [1] we have found that these distributions are, with good approximation, chi-squared probability distributions of the form

$$P_k(\lambda) = \frac{1}{\Gamma(\nu_k)} \frac{\nu_k}{\alpha_k} \left(\frac{\nu_k \lambda}{\alpha_k}\right)^{\nu_k - 1} \exp\left(-\frac{\nu_k \lambda}{\alpha_k}\right) \tag{5}$$

where $\Gamma(x)$ stands for the gamma function, and α_k and ν_k are external parameters [1].

To evaluate the probability distribution of a function $G(\lambda_1, \ldots, \lambda_d)$ of the eigenvalues—such as the asphericity, for example—one needs the combined probability distribution $Q(\lambda_1, \ldots, \lambda_r)$:

$$P_G(x) = \int_0^\infty d\lambda_1 \int_0^\infty d\lambda_2 \ldots \int_0^\infty d\lambda_r\, \delta(x - G(\lambda_1, \ldots)) Q(\lambda_1, \ldots, \lambda_r). \tag{6}$$

In general, the combined probability distribution Q is not known, and so it is not always possible to explicitly evaluate the distribution (6). Usually, it is assumed that the probability distributions for the different λ_k's are independent, that is,

$$Q(\lambda_1, \ldots, \lambda_r) = \prod_{k=1}^{r} P_k(\lambda_k). \tag{7}$$

The eigenvalue ratios

$$R_{ij} = \frac{\lambda_i}{\lambda_j} \qquad i \neq j \tag{8}$$

constitute a particular example of a function of the eigenvalues. As we shall see later, these quantities are of particular interest for describing the shapes of random walks in low d spaces, and especially for $d = 2$. For future reference, we are going to introduce here some related definitions and formulae.

Let $P_{R_{ij}}$ be the probability distribution of R_{ij}. Applying equation (6) to this case, and after some simple calculations, one obtains

$$P_{R_{ij}}(z) = \int_0^\infty u\, Q(u, zu)\, du \qquad 0 \leqslant z < \infty \tag{9}$$

where $Q(\lambda_j, \lambda_i)$ is the combined probability distribution of the eigenvalues λ_j and λ_i. If (7) and (5) hold, then $Q(\lambda_j, \lambda_i) = P_j(\lambda_j) P_i(\lambda_i)$ and the integral in (9) can be solved straightforwardly giving

$$P_{R_{ij}}(z) = \frac{\Gamma(\nu_i + \nu_j)}{\Gamma(\nu_i)\Gamma(\nu_j)} \left(\frac{\alpha_j \nu_i}{\alpha_i \nu_j}\right)^{\nu_i} \frac{z^{\nu_i - 1}}{\left(1 + \frac{\alpha_j \nu_i}{\alpha_i \nu_j} z\right)^{\nu_i + \nu_j}} \qquad 0 \leqslant z < \infty. \tag{10}$$

Hereinafter we shall take, for convenience and with no loss of generality, $i > j$†. With this assumption, and by construction, we have $\lambda_i \leqslant \lambda_j$ and so the true probability

† It is easy to demonstrate that $P_{R_{ji}}(z) = z^{-2} P_{R_{ij}}(z^{-1})$ for all $i \neq j$.

distribution for $P_{R_{ij}}(z)$ vanishes for $z > 1$. Since the distribution (10) is strictly positive for all $z > 0$ (even when $i > j$), it is clear that it cannot represent the true one in the general case. Nevertheless, $P_{R_{ij}}(z)$ from (10) with $z > 1$ is very small in all cases where (7) adequately represents the true combined probability distribution, and in such situations it is an acceptable approximation to the true distribution.

In [1] the region of validity of (7) is discussed, arriving at the conclusion that the probability distributions for two different eigenvalues λ_i and λ_j, are approximately independent when they present a non-significative overlap, and this happens for large d and for i much different from j. The arguments presented in [1] can be directly translated to the case of R_{ij}, and lead us to the conclusion that the region where (10) is a good approximation to the true one is defined by the conditions

$$d \to \infty \qquad i \gg j\,. \tag{11}$$

It is also possible to establish that in this limit the parameters α_i, ν_i, α_j and ν_j verify [1]:

$$\nu_i, \nu_j \gg 1 \qquad \frac{\alpha_j \nu_i}{\alpha_i \nu_j} \gg 1\,. \tag{12}$$

When this equation holds, it follows immediately that $P_{R_{ij}}(z)$ from (10) is vanishingly small for all $z > 1$, as mentioned previously.

3. The asphericity in the case $d = 2$

The analytic evaluation of the resulting probability distribution for the asphericity in the general d-dimensional case is a challenging problem even if one assumes that (7) and (5) hold. Nevertheless, in the particular case $d = 2$, where the asphericity (4) reduces to

$$A = \left(\frac{\lambda_1 - \lambda_2}{\lambda_1 + \lambda_2}\right)^2 \tag{13}$$

it is possible to evaluate analytically its probability distribution with the result [1]

$$P_A(x) = \frac{\Gamma(\nu_1+\nu_2)}{\Gamma(\nu_1)\Gamma(\nu_2)} \left(\frac{\nu_1}{\alpha_1}\right)^{\nu_1} \left(\frac{\nu_2}{\alpha_2}\right)^{\nu_2} \frac{1}{\sqrt{x}(1-\sqrt{x})^2} \times \left\{ \frac{[\beta(x)]^{1-\nu_2}}{\left[\frac{\nu_1}{\alpha_1} + \frac{\nu_2}{\alpha_2 \beta(x)}\right]^{\nu_1+\nu_2}} + \frac{[\beta(x)]^{1+\nu_2}}{\left[\frac{\nu_1}{\alpha_1} + \frac{\nu_2 \beta(x)}{\alpha_2}\right]^{\nu_1+\nu_2}} \right\} \tag{14}$$

where $0 \leqslant x \leqslant 1$, and $\beta(x)$ is defined as

$$\beta(x) = \frac{1-\sqrt{x}}{1+\sqrt{x}}\,. \tag{15}$$

When comparing this distribution against the Monte Carlo data, as we have done in [1], it is possible to see that both distributions differ significantly, especially for small values of x. For $x \to 0$ the true distribution takes non-zero finite values, while (14) diverges. This disagreement is mainly due to the lack of independence between the distributions for λ_1 and λ_2 [1].

Here we are going to study the analytical form of the two-dimensional asphericity probability distribution. To this end, we observe that A is connected to the ratio R_{21} via

$$A = \left(\frac{1-R_{21}}{1+R_{21}}\right)^2. \tag{16}$$

Therefore, in the two-dimensional case the asphericity can be related to a single quantity—the ratio R_{21}—and then if one knows $P_{R_{21}}(z)$, the probability distribution $P_A(x)$ can be evaluated easily. In fact, a simple and straightforward calculation leads us to

$$P_A(x) = \frac{1}{\sqrt{x}(1-x)}\left[\beta(x)P_{R_{21}}(\beta(x)) + \frac{1}{\beta(x)}P_{R_{21}}\left(\frac{1}{\beta(x)}\right)\right] \qquad 0 \leqslant x \leqslant 1 . \tag{17}$$

Notice that if $P_{R_{21}}$ from (10) is placed into (17), then (14) is obtained, this being an internal consistency check of these distributions. On the other hand, if $P_{R_{21}}(z)$ is null for $z > 1$, then the second term in (17) vanishes identically (notice that $0 \leqslant \beta \leqslant 1$ when $0 \leqslant x \leqslant 1$), and one gets

$$P_A(x) = \frac{1}{\sqrt{x}(1+\sqrt{x})^2}P_{R_{21}}(\beta(x)) . \tag{18}$$

Of course, these equations are only valid in the $d = 2$ case; for $d > 2$ the asphericity does depend on more than a single eigenvalue ratio. The probability distribution $P_{R_{ij}}$, however, can be studied in the general d case. For this reason it is more convenient to study the first term of this distribution and then use (18) to obtain the resulting distribution for the asphericity. This is what we will do in the following sections.

4. The probability distribution for the ratios R_{ij}

The distribution (10) was obtained assuming independence between the probability distributions of λ_i and λ_j. As discussed in section 2, equation (10) is a good approximation to the true distribution in the limit (11). We can therefore consider that the distribution (10) represents the asymptotic limit of the true one when $d \gg 1$ and $i \gg j$. We also recall that we are considering $i > j$ so the true distribution must vanish identically for $z > 1$. Furthermore, it is not difficult to realize (see, for example, [9]) that for sufficiently large s, also $P_{R_{ij}}(1)$ is equal to zero.

If we are looking for an approximation to the true distribution, we must consider just those functions which verify all the mentioned *necessary* conditions, namely: (i) it is zero for $z \geqslant 1$, and (ii) it tends asymptotically to (10) in the limit (11). Of course, additional conditions must be imposed in order to completely determine the correct distribution. A usual approach in this direction is to build a parametrized function which verifies all the necessary requirements for certain parameter ranges, and then adjust the parameters imposing the additional constraint (or set of constraints) of fitting some given simulation (or experimental) data.

One such distribution is the following:

$$P_{R_{ij}}(z) = \begin{cases} \dfrac{1}{U}\dfrac{z^{\omega-1}(1-z)^{\gamma-1}}{(1+az)^{\omega+\omega'}} & 0 \leqslant z \leqslant 1 \\ 0 & z > 1 \end{cases} \tag{19}$$

where ω, ω', γ and a are external parameters, and U is a normalizing constant which can be evaluated imposing the usual normalization condition:

$$U = \int_0^1 \frac{z^{\omega-1}(1-z)^{\gamma-1}}{(1+az)^{\omega+\omega'}}\,dz . \tag{20}$$

The integral in (20) can be evaluated analytically [10], and after some algebra the constant U can be put in the form

$$U = \frac{\Gamma(\gamma)\Gamma(\omega)}{\Gamma(\gamma+\omega)}(1+a)^{-\omega}F\left(\gamma-\omega', \omega; \gamma+\omega; \frac{a}{1+a}\right) \tag{21}$$

where the function $F(\alpha, \beta; \gamma; z)$ is the well known hypergeometric function defined as

$$F(\alpha, \beta; \gamma; z) = 1 + \frac{\alpha\beta}{\gamma}\frac{z}{1!} + \frac{\alpha(\alpha+1)\beta(\beta+1)}{\gamma(\gamma+1)}\frac{z^2}{2!} + \cdots \tag{22}$$

with $|z| < 1$.

In order to ensure that (19) has all the necessary properties mentioned, we must impose the following restrictions to the values that the external parameters can take:

$$\omega > 1 \qquad \omega' \geqslant 0 \qquad \gamma > 1 \qquad a > 0 \tag{23}$$

and these parameters should approach the following limits asymptotically for $d \to \infty$ and $i \gg j$:

$$\begin{aligned} &\omega \to \nu_i \qquad \omega' \to \nu_j \\ &\gamma \to 1 \qquad a \to (\alpha_j \nu_i)/(\alpha_i \nu_j)\,. \end{aligned} \tag{24}$$

It is not difficult to see that when (23) and (24) hold, the necessary conditions (i) and (ii) are satisfied. In fact (i) is satisfied trivially. To see that (ii) holds it is also necessary to take into account that while in (19) $P_{R_{ij}}(z) = 0$ for $z \geqslant 1$, the distribution (10) is positive for all $z > 0$. To show that the two distributions are approximately equivalent in the asymptotic limit, one must require that $P_{R_{ij}}(z)$ in (10) be vanishingly small for all $z \geqslant 1$. This can be ensured since from (12) we can write

$$\frac{\alpha_j \nu_i}{\alpha_i \nu_j} = a \simeq (1 + a) \gg 1\,. \tag{25}$$

With this additional result, using the following property of the hypergeometric function:

$$F\left(\gamma - \omega', \omega; \gamma + \omega; \frac{a}{1+a}\right) \simeq F(1 - \omega', \omega; 1 + \omega; 1) = \frac{\Gamma(\omega+1)\Gamma(\omega')}{\Gamma(\omega+\omega')} \tag{26}$$

and performing some simple algebra, it is easy to prove the equivalence of both distributions, that is, that the condition (ii) holds.

Therefore, the distribution (19) verifies all the necessary conditions that can be required *a priori*. In order to check the validity of (19) to adequately represent the true distribution in a particular case, we are going to determine the external parameters with the help of nonlinear least-squares fits to Monte Carlo data, as we shall see in the next section.

4.1. Test of the distribution (19)

We have performed many Monte Carlo simulations obtaining frequency histograms for several ratios R_{ij}. The simulations were done similarly as explained in [1]. A certain number N of independent random walks were generated. For each random walk, the inertia matrix (3) and the corresponding eigenvalues $\lambda_1, \ldots, \lambda_d$ were calculated. Then these data were used to build frequency histograms in the following way. (i) A certain number m of intervals $[x_k, x_{k+1})$, $k = 1, \ldots, m$ ($x_k > x_l$ for $k > l$) were defined such that $[x_1, x_{m+1}]$ represents the region of interest for the corresponding variable ($x_1 = 0$ and $x_{m+1} = 1$ in the cases of R_{ij} and A). (ii) The N Monte Carlo samples are used to evaluate the m frequencies f_k, $k = 1, \ldots, m$, which represent the number of times the variable happened to lie in the corresponding interval $[x_k, x_{k+1})$. The f_k's are modified to obtain normalized frequencies h_k in the following way:

$$h_k = \frac{f_k}{N(x_{k+1} - x_k)} \qquad k = 1, \ldots, m\,. \tag{27}$$

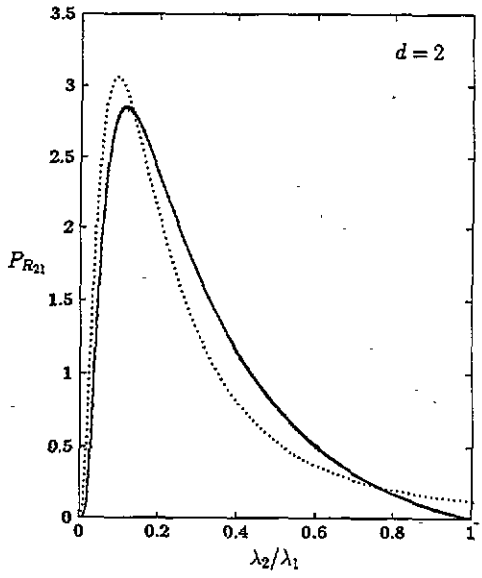

Figure 1. Probability distribution of the eigenvalue ratio R_{21}, in the $d = 2$, $s = 100$ case. The histogram corresponds to normalized Monte Carlo data with $N = 10^8$ and $m = 2000$. The full curve (not very distinguishable from the Monte Carlo histogram) corresponds to distribution (19) with parameters obtained with a nonlinear least-squares fit to the Monte Carlo data. The dotted curve represents (10) with parameters calculated as described in [1].

The relation between these frequencies and an analytical probability distribution $P(x)$ follows immediately. For N large we can equate f_k to $N\int_{x_k}^{x_{k+1}} P(x)\,dx$, and therefore

$$h_k \leftrightarrow \frac{1}{x_{k+1}-x_k}\int_{x_k}^{x_{k+1}} P(x)\,dx = P(\xi_k)\,. \tag{28}$$

for some $\xi_k \in [x_k, x_{k+1}]$. If m is large, the intervals $[x_k, x_{k+1}]$ are small and ξ_k can be approximated satisfactorily by

$$\xi_k = \frac{x_{k+1}+x_k}{2}\,. \tag{29}$$

The simulations presented here were performed using very large values of N and m (superior by more than one order of magnitude to the corresponding ones used in [1]), and therefore permit the safe use of (28) and (29).

In the case of the ratios R_{ij}, we have performed simulations in spaces of different dimensions d, keeping s fixed, generally equal to 100 (we have not detected significant changes in the distributions for larger values of s).

In figures 1–4, data corresponding to the cases $d = 2$, 3, 6, and 30, respectively, is displayed. In all these figures we have plotted three curves, namely: (i) the Monte Carlo normalized histogram (full curve). (ii) $P_{R_{ij}}$ from (19) (full curves), with parameters ω, ω', γ and a obtained from a nonlinear least-squares fit of the distribution to the Monte Carlo data. The well known Levenberg–Marquardt algorithm [11] was used to perform the fit. (iii) $P_{R_{ij}}$ from (10) (dotted curves), with parameters α_i, ν_i, α_j and ν_j obtained from other independent Monte Carlo simulations as explained in [1].

In table 1 we display some representative values of the parameters used in the plots. As mentioned, the parameters corresponding to the distribution (19) were obtained from nonlinear least-squares fits, while the ones corresponding to the asymptotic distribution (10) were calculated with the method of our previous work (see [1], table 2). We can clearly see the excellent agreement between the true distribution and (19) (in most cases it is not possible to distinguish between plots (i) and (ii)), for all values of d, i and j considered. The difference between the curves (i) and (ii) is always smaller than the average noise of

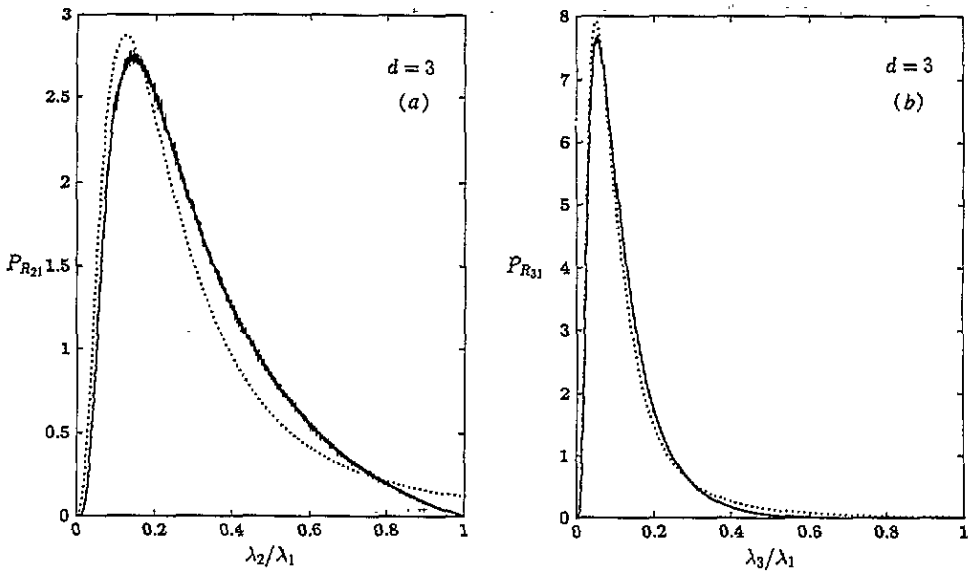

Figure 2. Same as figure 1, but in the $d = 3$ case with $N = 10^7$ and displaying the ratios (*a*) R_{21} and (*b*) R_{31}.

Table 1. Representative values of parameters corresponding to the probability distribution (19) for different ratios $R_{i1} = \lambda_i/\lambda_1$, as obtained from nonlinear least squares fits of (19) to the respective Monte Carlo data. The parameters corresponding to the asymptotic distribution (10) are also listed.

d	i	ω	ν_i	ω'	ν_1	γ	a	$(\alpha_1\nu_i)/(\alpha_i\nu_1)$
2	2	6.68	3.22	0.28	1.92	2.12	33.47	8.28
3	2	10.29	4.13	0.50	2.49	2.04	38.50	7.32
6	2	12.86	6.03	1.73	4.03	1.87	23.56	6.11
30	2	20.47	17.83	13.46	16.19	1.68	5.92	4.39
30	6	39.76	42.42	16.29	16.19	1.11	88.49	95.02

the Monte Carlo data. It is also possible to notice that the asymptotic distribution (10) separates significantly from the true one in the low d cases, and approaches it when d is large and/or $i \gg j$. Compare, for example, figures 2(*a*) and (*b*), and figures 3(*a*)–(*c*).

In the $d = 30$ case, the two distributions (10) and (19) do not differ significantly. This also shows up in the values of the parameters obtained from the least-squares fit, especially for R_{61}, which are approximately equal to the corresponding asymptotic values of (24) (see table 1).

We have also performed simulations for many other ratios R_{ij} in a variety of situations obtaining qualitatively similar results. Since we were not able to find previous papers studying the probability distributions of the ratios R_{ij}, we cannot present comparisons with independent calculations.

There do exist, however, studies of the ratios of *mean values* [4, 7]:

$$r_{ij} = \frac{\langle\lambda_i\rangle}{\langle\lambda_j\rangle} \tag{30}$$

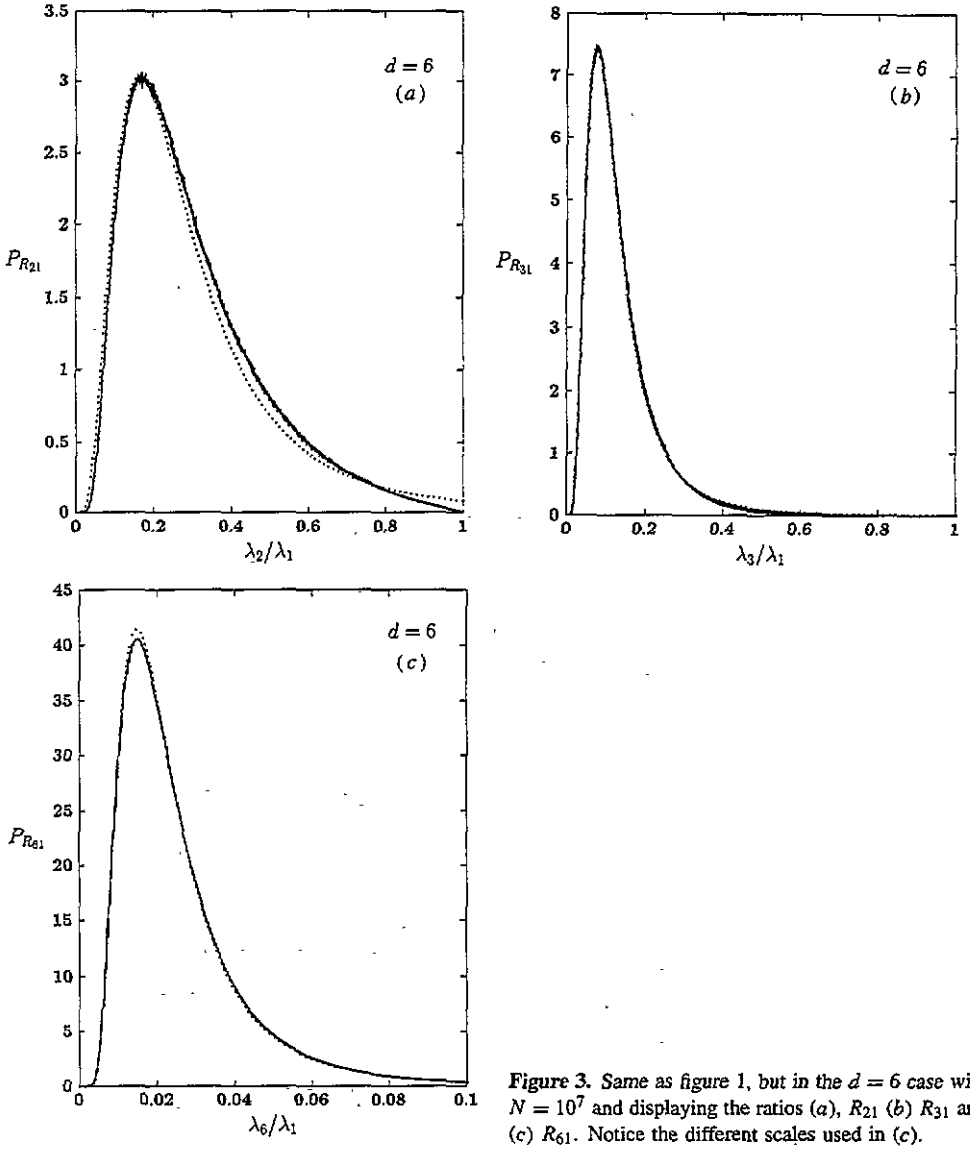

Figure 3. *Same as figure 1, but in the $d = 6$ case with $N = 10^7$ and displaying the ratios (a), R_{21} (b) R_{31} and (c) R_{61}. Notice the different scales used in (c).*

and of the mean values $\langle\lambda_i\rangle$ [1, 8] which can be used to evaluate the corresponding ratios r_{ij}. Of course, the quantities R_{ij} and r_{ij} are conceptually different and there is no direct way of comparing them. Nevertheless, the ratios r_{ij} and the respective mean values $\langle R_{ij}\rangle$ should be of the same order of magnitude, and so a comparison between them can be considered as an additional check of the validity of distribution (19).

In order to evaluate $\langle R_{ij}\rangle$, it is necessary to calculate the integral

$$\langle R_{ij}\rangle = \int_0^1 z\, P_{R_{ij}}(z)\, dz. \tag{31}$$

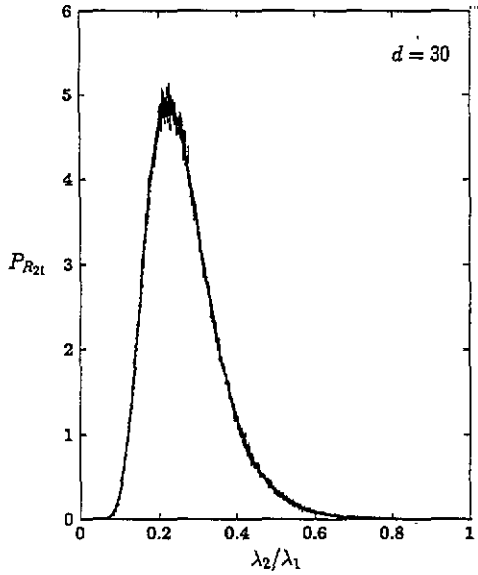

Figure 4. Same as figure 1, but in the $d = 30$ case with $N = 10^6$. In this case the three curves, namely, the Monte Carlo normalized histogram and distributions (19) and (10) are coincident.

Similarly as for the evaluation of (21), we can evaluate, for $n = 1, 2, \ldots$, the nth moment of distribution (19) [10]:

$$\langle R_{ij}^n \rangle = \frac{1}{U} \int_0^1 \frac{z^{n+\omega-1}(1-z)^{\gamma-1}}{(1+az)^{\omega+\omega'}} \, dz$$
$$= \frac{1}{(1+a)^n} \left[\prod_{k=0}^{n-1} \frac{(\omega+k)}{(\gamma+\omega+k)} \right] \frac{F(\gamma-\omega'+n,\ \omega+n;\ \gamma+\omega+n;\ b)}{F(\gamma-\omega',\ \omega;\ \gamma+\omega;\ b)} \tag{32}$$

with $b = a/(1+a)$. $\langle R_{ij} \rangle$ is then obtained setting $n = 1$:

$$\langle R_{ij} \rangle = \frac{\omega}{(1+a)(\gamma+\omega)} \frac{F(\gamma-\omega'+1,\ \omega+1;\ \gamma+\omega+1;\ b)}{F(\gamma-\omega',\ \omega;\ \gamma+\omega;\ b)}. \tag{33}$$

Some typical values for the ratios r_{ij} are given in [4]. Here, as well as in [7], only the $d = 3$ case is considered, and it is reported that for s very large the ratios r_{13} and r_{23} are equal to 12.0 and 2.73, respectively. It is also said that these values are in good agreement with the results obtained in [7], and that they do not depend strongly on s. From these numbers, it is easy to obtain the following ratios r_{ij} with $i > j$: $r_{21} = 0.228$ and $r_{31} = 0.083$. These values should be contrasted with the corresponding ones for $\langle R_{ij} \rangle$ coming from (33) with the external parameters taken from the solution of the least-squares fit, which in the $d = 3$, $s = 100$ case are the following: $\langle R_{21} \rangle = 0.301$ and $\langle R_{31} \rangle = 0.117$. It is evident that there is a good qualitative agreement between both pairs of numbers.

From the results reported in [1] for the mean values $\langle \lambda_1 \rangle$ and their respective errors, and the characteristics of the different probability distributions (equation (5) in this paper), it is possible to make the following considerations. (i) For large d the standard deviations of all the quantities considered are very small and so r_{ij} and $\langle R_{ij} \rangle$ should not present large differences. This can be confirmed analysing some results for $d = 30$, $s = 100$. Using the data tabulated in [1] we can calculate, for instance: $r_{61} = 0.027\,577 \pm 0.000\,057$. From equation (33), and using the data of table 1, one obtains $\langle R_{61} \rangle = 0.0294$. It is evident that in this case the difference between r_{ij} and $\langle R_{ij} \rangle$ is less significant than in the $d = 3$ case of the preceding paragraph. (ii) We can see that $\langle R_{ij} \rangle > r_{ij}$ in all the

examples that were considered. This can be explained qualitatively in the following way. Looking at the probability distributions $P_i(\lambda)$ displayed in [1], it is evident that the most probable value λ_{mp} is always less than the respective mean value $\langle\lambda\rangle$, and that the relative difference $(\langle\lambda\rangle - \lambda_{mp})/\langle\lambda\rangle$ decreases when the label i is increased. A direct inspection of the different probability distributions shows that the mean value of R_{ij} is approximately equal to $\lambda_{mp_i}/\lambda_{mp_j}$ $(i > j)$. Therefore we have $\langle R_{i1}\rangle \simeq \lambda_{mp_i}/\lambda_{mp_1} > \langle\lambda_i\rangle/\langle\lambda_1\rangle$, as expected.

Both the results of the Monte Carlo simulations and the comparisons with related quantities here presented give strong support to the conclusion that the probability distribution of all the ratios R_{ij} $(i > j)$ can be approximated adequately in the form of (19).

5. Back to the asphericity in the case $d = 2$

As established in section 3, the probability distribution for A in $d = 2$ is related to the probability distribution of the ratio R_{21}. Considering the experimental evidence presented in section 4, we can assume that $P_{R_{21}}$ is of the form of (19). Then, replacing this distribution into (18) and performing some simple algebra, one obtains the corresponding distribution for the asphericity:

$$P_A(x) = \frac{2^{\gamma-1}}{U} \frac{(\sqrt{x})^{\gamma-2}(1-\sqrt{x})^{\omega-1}}{(1+\sqrt{x})^{2-\omega'}\left[(a+1)-(a-1)\sqrt{x}\right]^{\omega+\omega'}}. \tag{34}$$

We have performed an independent Monte Carlo simulation to obtain a frequency histogram for the asphericity in the case $d = 2$ and $s = 100$. We used this data, normalized accordingly with (27), to see the correspondence of (34) with the true distribution, and, at the same time, to check the global consistency of the present approach.

The data has been plotted in figure 5. The histogram corresponds to the normalized Monte Carlo data, the full continuous line correspond to distribution (34) with ω, ω', γ and a taken from the data of table 1 (we have not performed any fit using the asphericity data), and the dotted curve represents distribution (14). Notice that this figure is a high-resolution

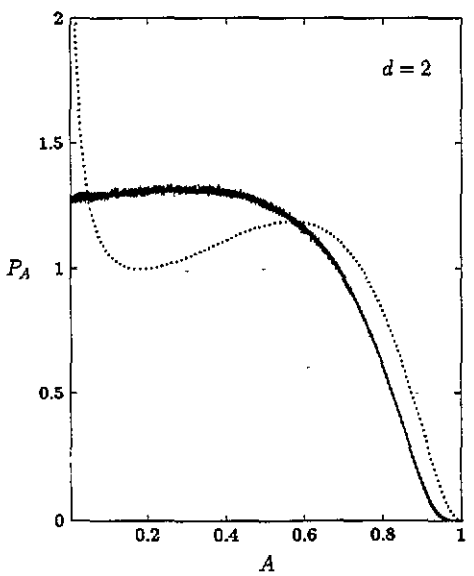

Figure 5. Probability distribution of the asphericity in the $d = 2$, $s = 100$ case. The histogram corresponds to normalized Monte Carlo data with $N = 10^8$ and $m = 5000$. The continuous full curve (not very distinguishable from the Monte Carlo histogram) corresponds to distribution (34) with parameters obtained with a nonlinear least-squares fit to the Monte Carlo data. The dotted curve represents equation (14) with parameters calculated as described in [1].

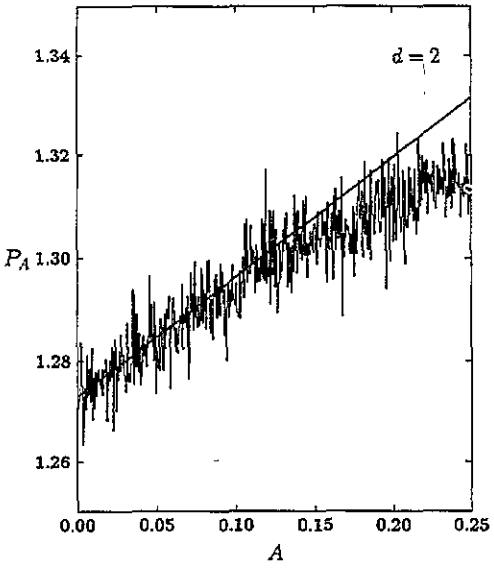

Figure 6. Detailed plot of the Monte Carlo histogram of figure 5, showing clearly that both $P_A(x)$ and $P'_A(x)$ are finite and positive for $x \to 0$. The straight line is a least-squares fit to the Monte Carlo data for $x \in [0, 0.05]$, and its equation is $y = 1.273 + 0.233\,x$.

version of figure 6(a) of [1].

It is evident that the distribution (34) and the Monte Carlo data are in very good agreement, except perhaps near the origin where both curves differ slightly.

Notice that from (34) we have $P_A(0) = 0$ for $\gamma > 2$. If we let $\gamma = 2$, we obtain

$$P_A(x) = \frac{2}{U} \frac{(1-\sqrt{x})^{\omega-1}}{(1+\sqrt{x})^{2-\omega'}\left[(a+1)-(a-1)\sqrt{x}\right]^{\omega+\omega'}} \tag{35}$$

and so in this case $P_A(0) = 2/[U(a+1)^{\omega+\omega'}] \neq 0$. We have therefore a critical behaviour of $P_A(x)$ in the neighbourhood of $\gamma = 2$. Looking closely at the Monte Carlo data corresponding to $x \to 0$, one can establish that $P_A(0)$ and the derivative $P'_A(0)$ are both finite and positive. In fact, in figure 6 we have displayed a small portion of the Monte Carlo histogram of figure 5. We can see that $P_A(x) \neq 0$ for x as small as $m^{-1} = 2 \times 10^{-4}$. The straight line of figure 6 is a least-squares fit to the Monte Carlo data for $x \leqslant 0.05$, and indicates clearly that $P'_A(0) > 0$†.

It is worthwhile mentioning, however, that if a least-squares fit for $P_{R_{21}}$ is performed keeping γ fixed and equal to 2, the resulting probability distributions obtained for both R_{21} and A (equation (35)) do not approximate the respective Monte Carlo data as well as the distributions plotted in figures 1 and 5 do. This fact indicates that some small corrections to (19) may be needed in order to obtain probability distributions that will improve the ones here presented, especially in the $d = 2$ case and for $P_A(x)$ with $x \to 0$.

6. Conclusions and final remarks

We have performed a study of the probability distributions of the ratios of principal inertia moments, R_{ij}, in arbitrary dimensions and of the asphericity, A, in two-dimensional

† The fact that $P'_A(0) > 0$ indicates that the distribution $P_A(x)$ possesses a maximum for some $x \neq 0$. In fact, looking at figure 5 one can see that the maximum is placed at $x \simeq 0.3$. This is made evident mainly for the low level of noise of the histogram, due to the very large number of samples used in the Monte Carlo simulations. Notice that in an earlier reference to the probability distribution of the two-dimensional asphericity [3] it was reported that its most probable value is placed at $x = 0$, which is not compatible with the results of our simulation.

spaces. We have analysed the connection existing between both quantities and compared the corresponding analytical distributions with Monte Carlo data.

From knowledge of the analytical form of the probability distribution for the moment ratios in the asymptotic limit for large dimension and negligible overlap between eigenvalue distributions [1] ($d \gg 1$ and $i \gg j$) (equation (10)), it was possible to construct heuristically a generalization in order to obtain a four-parameter analytical expression for the distribution in the general case (equation (19)). Performing nonlinear least-squares fits to Monte Carlo data in order to evaluate the external parameters at each case, it was possible to show that the distribution obtained agrees excellently with the Monte Carlo data, and that the external parameters possess the expected behaviour in the case of large spatial dimension.

Using the mentioned distribution (19) in the case of two-dimensional spaces, it was possible to obtain an analytical expression for the asphericity (equation (34)), which also presents a very good agreement with the corresponding Monte Carlo data. However, both distributions differ slightly in the neighbourhood of the origin, suggesting that some secondary corrections would be needed in order to improve the accuracy of distribution (34).

Acknowledgments

We are indebted to J L Alessandrini for helpful comments and suggestions. We are grateful to Fundación Antorchas of Argentina for its help and financial support. This work was partially supported by the Consejo Nacional de Investigaciones Científicas y Técnicas of Argentina.

References

[1] Sciutto S J 1994 *J. Phys. A: Math. Gen.* **27** 7015
[2] Rudnick J and Gaspari G 1986 *J. Phys. A: Math. Gen.* **19** L191
[3] Jagodzinski O, Eisenriegler E and Kremer K 1992 *J. Physique I* **2** 2243
[4] Bruns W 1992 *Makromol. Chem. Theory. Simul.* **1** 287
[5] Szleifer I 1992 *J. Chem. Phys.* **92** 6940
[6] Alessandrini J L and Vila J 1994 *Phys. Rev.* E **49** R3584
[7] Šolc K and Stockmayer W H 1971 *J. Chem. Phys.* **54** 2756
Šolc K 1971 *J. Chem. Phys.* **55** 335
[8] Gaspari G, Rudnick J and Beldjenna A 1987 *J. Phys. A: Math. Gen.* **20** 3393
[9] Šolc K and Gobush W 1974 *Macromolecules* **7** 814
[10] The integral can be found in most tables of integrals. See, for example, Gradshteyn I S and Ryzhik I M 1980 *Table of Integrals, Series and Products* (New York: Academic)
[11] The nonlinear least-squares fits were performed using a routine of the public domain package MINPACK of the numerical software library NETLIB. This software can be obtained sending electronic mail to `netlib@research.att.com`.